

Polymer Chemistry

Accepted Manuscript



This is an *Accepted Manuscript*, which has been through the Royal Society of Chemistry peer review process and has been accepted for publication.

Accepted Manuscripts are published online shortly after acceptance, before technical editing, formatting and proof reading. Using this free service, authors can make their results available to the community, in citable form, before we publish the edited article. We will replace this *Accepted Manuscript* with the edited and formatted *Advance Article* as soon as it is available.

You can find more information about *Accepted Manuscripts* in the [Information for Authors](#).

Please note that technical editing may introduce minor changes to the text and/or graphics, which may alter content. The journal's standard [Terms & Conditions](#) and the [Ethical guidelines](#) still apply. In no event shall the Royal Society of Chemistry be held responsible for any errors or omissions in this *Accepted Manuscript* or any consequences arising from the use of any information it contains.

ARTICLE

Modular design of profluorescent polymer sensors

Cite this: DOI: 10.1039/x0xx00000x

Emily Simpson,^a Zoran Ristovski^a, Steven E. Bottle^a, Kathryn E. Fairfull-Smith^a and James P. Blinco^{a*}

Received 00th January 2012,
Accepted 00th January 2012

DOI: 10.1039/x0xx00000x

www.rsc.org/

A simple modular strategy for the synthesis of profluorescent nitroxide containing polymers is described. The incorporation of an epoxide as a pendant functionality on a polymer backbone synthesized using ATRP and subsequent nucleophilic ring-opening with sodium azide gave hydroxyl and azide functionality within a 3-bond radius. Orthogonal coupling chemistry then allowed the independent attachment of fluorophore and nitroxide groups in close proximity, giving rise to a profluorescent polymer. Validation of the viability of these materials as fluorescent sensors is demonstrated through efficient fluorescence switch-on observed when the materials are exposed to a model reductant or carbon-centred radical source.

Introduction

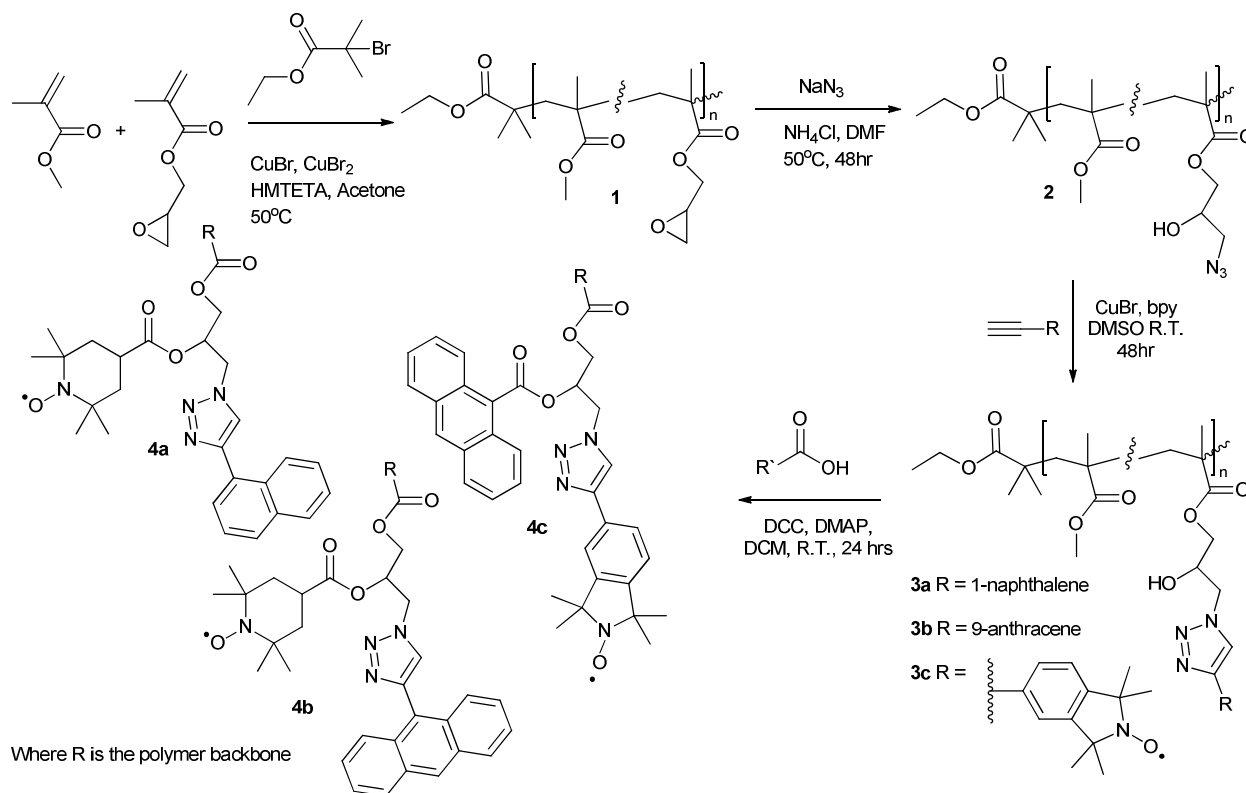
Nitroxides are stable, kinetically persistent free radicals that possess a number of remarkable physical and chemical properties which parallel those found in less stable free radical compounds. These broad-ranging properties explain why nitroxides have found applications in a wide variety of fields including controlled free radical polymerisation,^{1,2} biological-³ and material-based antioxidants⁴ and Electron Paramagnetic Resonance (EPR) spectroscopy/imaging.⁵ Nitroxides are excellent quenchers of the excited electronic states of a wide variety of fluorescent molecules. This quenching effect can occur both inter- and intra-molecularly and the mechanism is based on electron exchange interactions between the paramagnetic species and the excited-state fluorophore. Based on this quenching, nitroxides have found increasing use as fluorescence-response based chemosensors for radical species within the environment.⁶ It is now well established that there is a clear correlation between acute and chronic human health impacts (eg. the genesis of pulmonary and cardiovascular injury as well as specific cancers) and exposure to airborne fine particles.⁷⁻¹² Reactive oxygen species (ROS) and related free radicals are considered to be key components underpinning the various adverse health effects associated with exposure to ambient particulate matter.¹³ Therefore, measurement of these reactive species is a crucial factor for assessing the potential toxicity of particulates.

A number of groups around the world have investigated small molecule profluorescent nitroxides as sensors of gas phase

radical species arising from diesel exhaust,^{14,15} cigarette smoke^{16,17} and combustion of other bio-masses.¹⁸ These systems have also been used to investigate reactive radical species formed through photolysis of particulates in waters from natural sources.¹⁹ The “switch-on” fluorescence technique exploited in profluorescent nitroxide systems represents a powerful analytical tool. To date however, profluorescent nitroxide probes have all been small molecule compounds dissolved in an appropriate solvent. In the examples of monitoring gas phase radicals, the samples had to be bubbled through an organic solvent solution containing the profluorescent nitroxide probe. This involves an extra layer of sampling complexity and introduces additional preparation steps between sample collection and quantification of the trapped radical adducts. This is particularly problematic if the analogues are unstable and have a propensity to undergo subsequent reactions. Recently, Sleiman *et al.* demonstrated that it was possible to move to a solid supported system just by physically coating glass beads with a profluorescent nitroxide. This approach leads to improved probe and radical adducts stability and gives the minimum interference from ozone and NO_x.²⁰ In a flow-through monitoring systems however, simple physical coating may lead to leaching of some of the probe during sampling.

Another consideration when employing small molecule profluorescent nitroxide probes is that their synthesis can be demanding and somewhat inefficient.²¹⁻²⁵ Furthermore, depending on the application in which the profluorescent nitroxide is being exploited, it may be desirable to tune the

properties of the fluorophore (e.g. excitation/emission wavelengths) or the nitroxide (e.g. redox potential). This would lead to individual, multi-step synthesis for each new



Scheme 1 Synthetic route used to access profluorescent polymer sensors **4a-c**

profluorescent nitroxide contemplated for the application. Knall *et. al.* have shown recently that it is possible to produce a polymer via ROMP that exhibits some profluorescent capabilities by including both a fluorophore and nitroxide adorned monomer unit.²⁶ This allows a combinatorial approach to production of profluorescent nitroxide probes and has the added advantage in allowing additional properties (water solubility, biocompatibility) to be incorporated through the addition of other monomer units to the polymer. However, the random nature of the copolymerisation means there is no guarantee of nitroxide and fluorophore proximity. Proximity is a key criteria controlling fluorescence quenching by nitroxides with the greatest effect being observed when the moieties are within 0–2.5 nm of each other.²⁷

Herein, we describe a simple methodology that allows the modular synthesis of highly sensitive, profluorescent nitroxide polymers. Our approach incorporates glycidyl methacrylate into the polymer backbone which, upon oxirane ring opening, generates azide and alcohol functionalities in close proximity.²⁸ By then employing orthogonal coupling techniques, it is possible to produce profluorescent nitroxide polymers with sensitivities akin to the equivalent small molecule analogues. Using this approach there is the potential to produce a number of profluorescent polymers from a single polymer backbone. By coupling the appropriate fluorophore to the polymer,

targeted fluorescence properties can be given to the probe material. As a proof of concept, model redox and radical trapping reactions were undertaken to demonstrate the ability of the polymers to function as sensor materials.

Experimental Section

Materials

Methyl methacrylate (99%, Sigma) and glycidyl methacrylate (97%, Sigma) had inhibitor removed by passing through a column of aluminium oxide 90 active basic (particle size: 0.063–0.200 mm). Copper bromide was purified with glacial acetic acid and washed with pure ethanol, then stored under argon. 1-Ethynyl naphthalene,²⁹ 9-ethynyl anthracene³⁰ and 5-ethynyl-1,1,3,3-tetramethylisoindolin-2-yl³¹ were prepared as described in previous publications. Liquid chromatography grade THF was used as solvent for all UV-Vis and fluorescence spectroscopy measurements. All other reagents were of analytical reagent grade purity, or higher, and used as received.

Instrumentation

NMR spectra were recorded on a Bruker Avance 400 spectrometer and referenced to the relevant solvent peak. Size Exclusion Chromatography (SEC) was performed using a Waters SEC system equipped with a Waters 2487 dual wavelength absorbance detector (operating at 300 and 350 nm)

and a Waters 2414 refractive index detector connected in series. Three consecutive Phenomenex Phenogel 5 μ columns (104 Å, 103 Å, 50 Å), preceded by a guard column, were used. The system was operated at 30°C using tetrahydrofuran as eluent at a flow rate of 1 mL min⁻¹. A 7-point calibration using polystyrene standards (1.35 \times 10³ – 3.821 \times 10⁵ g mol⁻¹) was used to obtain molecular weights and polydispersities. Ultraviolet-Visible spectra, with a spectral range of 250-500 nm were acquired using a Varian Cary 3000 UV-Visible spectrophotometer. Fluorescence emission spectra were collected using a Varian Cary Eclipse fluorescence spectrophotometer. Fourier transform infrared (FTIR) spectra were recorded on a Fourier Transform Infrared Spectrometer equipped with a DTGS TEC detector and an ATR objective. EPR spectroscopy was carried out on a MiniScope EPR spectrometer. Samples were dissolved in THF ~~water~~ and the spectra were recorded at 22°C. Full NMR, IR, UV-Vis, Fluorescence and EPR (where applicable) can be found in the supporting information.

Poly(methyl methacrylate-co-glycidyl methacrylate) (1)

Methyl methacrylate (4 g, 40 mmol), CuBr (14.5 mg, 0.1 mmol) and CuBr₂ (5.7 mg, 0.025 mmol) were dissolved in acetone, sealed and deoxygenated by bubbling with argon for 20 minutes. The flask was then evacuated and back-filled with nitrogen several times followed by the addition of deoxygenated HMTETA (68 μ L, 0.25 mmol). The mixture was heated to 50 °C and glycidyl methacrylate (1.42 g, 10 mmol) was added after the evidence of the catalyst complex being formed via distinctive colour change. The initiator, ethyl α -bromoisobutyrate (37 μ L, 0.25 mmol) was added and the reaction stirred for 240 minutes. The mixture was allowed to cool to room temperature and then the flask was opened to air to decompose the catalyst complex. The resulting solution was diluted with THF, passed through a neutral alumina column and twice precipitated by addition to hexanes. (yield = 3.2 g, 61%, conversion (NMR) 70%, M_n (GPC)=13400, $D=1.23$) ¹H NMR (400 MHz, CDCl₃) δ 0.85-2.00 (36H, m, CH₂, CH₃), δ 2.65 (1H, s, O-CH₂-CH), δ 2.87 (1H, s, O-CH₂-CH), δ 3.25 (1H, s, O-CH-CH₂), δ 3.60 (18H, s, O-CH₃), δ 3.80 (1H, br s, COO-CH₂-CH), δ 4.35 (1H, br s, COO-CH₂-CH).

Poly(methyl methacrylate-co-3-azido-2-hydroxypropyl methacrylate) (2)

Sodium azide (87 mg, 1.34 mmol, 3 equiv. per epoxide) and ammonium chloride (72 mg, 1.34 mmol) were added to solution of polymer 1 (1 g) in DMF (20 mL). The mixture was then stirred at 50 °C for 26 hours. After this time the reaction mixture was cooled to room temperature and directly precipitated into water. The recovered polymer was then redissolved in THF, precipitated into hexanes and dried under vacuum (yield 980 mg, conversion (NMR) >95%, M_n (GPC)=14200, $D=1.26$, ¹H NMR (400 MHz, CDCl₃) δ 0.85-2.00 (40H, m, CH₂, CH₃), 3.45 (2H, br s, CH-CH₂-N₃), δ 3.60 (18H, s, O-CH₃), 4.10 (3H, br s, O-CH₂-CH-OH).

Typical procedure for copper-catalyzed azide-alkyne cycloaddition reactions

Polymer 2 (400 mg) was dissolved in DMSO (8 mL) followed by the addition of CuBr (18 mg, 0.125 mmol, 0.25 equiv/azide) and bipyridine (40 mg, 0.25 mmol, 0.5 equiv/azide). The mixture was degassed via bubbling with argon for 20 minutes, followed by addition of the appropriate alkyne (0.6 mmol, 1.2 equiv/azide). The reaction then stirred at room temperature for 48 hours. The reaction mixture was then opened to atmosphere, diluted with THF and passed through a plug of neutral alumina to remove the catalyst. The resulting product was then purified by repeated (2x) precipitation into methanol.

Reaction of polymer 2 with 1-ethynyl naphthalene (3a)

This reaction yielded 325 mg of an off-white solid, conversion (NMR) >95%, M_n (GPC)=13700, $D=1.24$, NMR (400MHz, CDCl₃) δ 0.85-2.00 (38H, m, CH₂, CH₃), δ 3.60 (18H, s, O-CH₃), δ 4.00-4.68 (5H, br m), δ 7.25-8.50 (8H, br m, Ar-H). Covalent attachment *via* CuAAC was also confirmed via complete disappearance of the azide stretch (2100 cm⁻¹) in the IR spectrum. Incorporation of the fluorophore was confirmed by UV-Vis and Fluorescence spectroscopy (Figures S5-6).

Reaction of polymer 2 with 9-ethynyl anthracene (3b)

This reaction yielded 385 mg of an off-white solid, conversion (NMR) >95% M_n (GPC)=14400, $D=1.33$, NMR (400MHz, CDCl₃) δ 0.85-2.00 (39H, m, CH₂, CH₃), δ 3.60 (18H, s, O-CH₃), δ 4.00-4.75 (5H, br m), δ 7.25-8.75 (10H, br m, Ar-H). Covalent attachment *via* CuAAC was also confirmed via complete disappearance of the azide stretch (2100 cm⁻¹) in the IR spectrum. Incorporation of the fluorophore was confirmed by UV-Vis and Fluorescence spectroscopy (Figures S9-10).

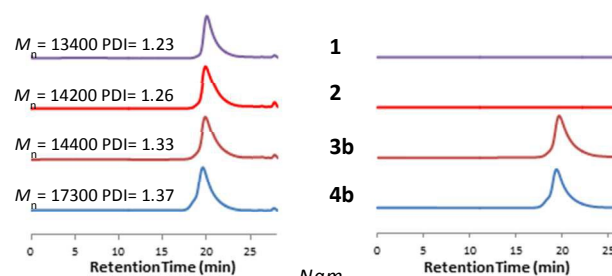
Reaction of polymer 2 with 5-ethynyl-1,1,3,3-tetramethylisindolin-2-yloxyl (3c)

This reaction yielded 260 mg of an off-white solid, NMR spectrum with broadened peaks was observed due to paramagnetic effects arising from the presence of the nitroxide groups (see SI Figure S12). M_n (GPC)=14200, $D=1.26$. Covalent attachment *via* CuAAC was also confirmed via complete disappearance of the azide stretch (2100 cm⁻¹) and appearance of the isindoline N-O[•] stretch (1435 cm⁻¹) in the IR spectrum (Figure S13). Incorporation of the free radical moiety was also confirmed *via* EPR spectroscopy ($G_2 = 1.972$, $\tau_R = 1.25 \times 10^{-9}$ s, Figure S14).

Typical procedure for DCC activated esterification

Polymer 3 (100 mg), the appropriate carboxylic acid derivative (2

equiv./alcohol), and 4-dimethylaminopy



ridine (1 equiv./alcohol) were dissolved in anhydrous dichloromethane (DCM) (5 mL) and the mixture degassed via argon bubbling for 20 minutes. This was followed by the addition of *N,N'*-dicyclohexycarbodiimide (DCC) and the cessation of the argon bubbling. The reaction was stirred for 24 hours whereupon the resultant white precipitate was removed by filtration. The filtrate was evaporated to dryness under reduced pressure and the resulting solid taken up in minimal THF (5 mL) and precipitated from methanol.

Reaction of polymer 3a with 4-carboxy-2,2,6,6-tetramethylpiperidine-*N*-oxyl (4a)

This reaction yielded 44 mg of an off-white solid that gave an NMR spectrum with broadened peaks due to paramagnetic effects arising from the presence of the nitroxide groups (See SI Figure S16), $M_n(\text{GPC})=19500$, $D=1.30$. Further evidence for the incorporation of the nitroxide moiety was given by the appearance of the piperidine N-O \cdot stretch (1435 cm^{-1}) in the IR spectrum (~~1364 cm^{-1}~~) and a characteristic 3 line nitroxide spectrum being detected by EPR ($G_2 = 1.973$, $\tau_R = 2.47 \times 10^{-10}\text{ s}$, Figure S17). UV-Vis spectroscopy still exhibited a strong, characteristic absorbance spectrum of the naphthalene chromophore but with the fluorescence emission substantially quenched (Figures S18-19) as expected from the influence of the nitroxide groups.

Reaction of polymer 3b with 4-carboxy-2,2,6,6-tetramethylpiperidine-*N*-oxyl (4b)

This reaction yielded 77 mg of an off-white solid that gave an NMR spectrum with broadened peaks due to paramagnetic effects arising from the presence of the nitroxide groups (See SI Figure S21), $M_n(\text{GPC})=17300$, $D=1.37$. Incorporation of the nitroxide moiety was shown by the appearance of the piperidine N-O \cdot stretch (1435 cm^{-1}) in the IR spectrum (~~1364 cm^{-1}~~) and a strong 3 line spectrum being recorded by EPR ($G_2 = 1.974$, $\tau_R = 4.12 \times 10^{-10}\text{ s}$, Figure S22). UV-Vis still exhibited a strong, characteristic anthracene chromophore absorbance but now with fluorescence substantially quenched (Figures S23-24).

Reaction of polymer 3c with 9-carboxyanthracene (4c)

This reaction yielded 53 mg of an off-white solid that gave an NMR spectrum with broadened peaks due to paramagnetic effects arising from the presence of the nitroxide groups (See SI Figure S26), $M_n(\text{GPC})=17000$, $D=1.35$. Incorporation of the anthracene moiety was demonstrated by the appearance of a strong characteristic absorbance in the UV-Vis spectrum (Figure S28). The proximity of the chromophore to the nitroxide is confirmed by the enhanced fluorescence quenching exhibited by the material (Figure S29).

Results and Discussion

Fig. 1 Comparison of the GPC elugrams for polymers **1**, **2**, **3b** and **4b** by both RI detection (left) and UV absorbance at 350nm (right). It can be seen that in all transformations there is minimal influence on the observed size of the polymer by RI. However, once the chromophore is introduced onto the backbone a marked change is observed on the UV trace.

Synthesis of all profluorescent nitroxide polymers was based on the four step reaction pathway that is outlined in Scheme 1. Initially, random co-polymerisation of methyl methacrylate and glycidyl methacrylate was undertaken using atom transfer radical polymerisation to give polymer **1**. An initial feed ratio of 5:1 MMA:GMA was chosen to ensure that in the final materials produced, the amount of intermolecular quenching from adjacent profluorescent nitroxide moieties would be minimised

The copolymer composition was determined using ^1H NMR spectroscopy by ratio of peak area of the methoxy protons at 3.60 ppm from the methyl methacrylate compared to the methine proton (3.25 ppm) arising from the glycidyl methacrylate. The molar ratio for composition was determined to be *ca.* 6:1 MMA:GMA. The epoxide functionality then underwent quantitative ring opening by sodium azide in the presence of ammonium chloride to give the dual functional polymer **2**, which was subsequently used as the backbone material for the construction of all the profluorescent nitroxide containing polymers. Incorporation of the azide moiety onto the polymer backbone was confirmed by IR spectroscopy through the characteristic absorption at 2100 cm^{-1} (See SI). The ^1H NMR spectrum showed characteristic changes³¹ such as a shift and coalescence of the methylene protons next to the ester with the methine proton at 4.1 ppm and also the appearance of the methylene protons next to the azide appearing at 3.45 ppm. Inspection of the GPC elugram showed a modest increase in molecular weight consistent with the addition of azide to the polymer. There was also no higher molecular weight species observed suggesting that no cross-linking of chains had occurred.

At this stage, either the nitroxide or the fluorophore could be attached to the polymer using a Copper Azide Alkyne Cycloaddition (CuAAC) reaction. Initially, 1-ethynyl naphthalene was reacted with **2** in the presence of CuBr catalyst to give polymer **3a**. Reaction was confirmed via complete disappearance of the azide absorption at 2100 cm^{-1} (See SI

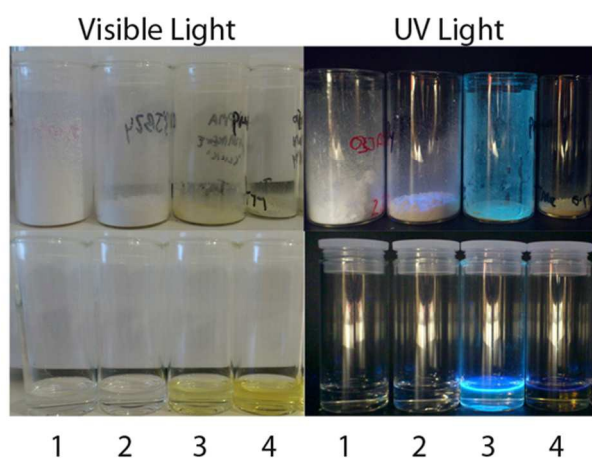


Fig. 2 Comparison of Polymers **1**, **2**, **3b** and **4b** under white light (left) and 350 nm UV light (right) in the solid state (top) and in THF solutions (bottom). While both **3b** and **4b** have an anthracene chromophore attached to the polymer only **3b** was fluorescent due to the effective quenching of the photoexcited state by the nitroxide also attached in polymer **4b**

Figure S13). The ^1H NMR (see SI Figure S5) spectrum showed substantial broadening of the signals associated with the methane and methylene protons associated with the reactive monomer unit, as well as the appearance of the naphthalene signals between 7.25 and 8.5 ppm. Comparison of the integration of the new naphthalene signals to the existing backbone indicated complete reaction of the starting material.

The signal from the triazole proton was not able to be distinguished from other signals in the NMR but given the significant broadening of the other signals, this is not unexpected. Coupling of the bulkier fluorophore (9-ethynyl anthracene) to polymer **2** also proceeded in a highly efficient manner to give polymer **3b**, and this demonstrated the value of the modular nature of the synthesis. The GPC elugram showed a very modest increase in the overall molecular weight of the polymer but the UV absorbance of the polymer increased substantially indicating the attachment of the chromophore to the polymer backbone (as shown in Figure 1). It was also possible to attach an alkynyl nitroxide to the polymer backbone using the same chemistry. CuAAC chemistries have previously been successfully employed on nitroxide containing small molecules.³³ In this case, NMR spectroscopy could not be used to estimate the success of the reaction due to the paramagnetic broadening effect of the nitroxide moiety. However, complete disappearance of the azide IR absorption was observed and a characteristic 3-line EPR signal was detected arising from the presence of the nitroxide group. Notably at this temperature and with this solvent, the observed EPR spectrum for **3c** is anisotropic and indicates some restricted movement of the nitroxide moiety (as demonstrated through the increase in rotational correlation time, τ_R , compared with the other spin containing polymers - See the SI Figure S14). To complete the synthesis of the profluorescent nitroxide containing polymer, a carboxy fluorophore/nitroxide was attached via esterification of

Table 1. Photophysical data for polymers **3a-c** and **4a-c**

Polymer	λ max (nm)	Fluorescence emission max (nm)	Φ_F
3a	294	352	0.277
3b	367	432	0.268
3c	-	-	-
4a	294	350	0.016
4b	367	426	0.026
4c	364	458	0.070

All samples were measured in THF at 25 °C. Quantum yield of fluorescence was calculated by comparison to an anthracene standard with a Φ_F of 0.33³³

the remaining alcohol functionality on the polymer backbone. While not used as extensively as the click chemistry for ligation, recently there have been several examples demonstrating the efficient nature in which esterification can be employed on ring-opened oxiranes attached to macromolecules.³⁴⁻³⁶ For polymers **3a** and **3b** 4-carboxy-2,2,6,6-tetramethylpiperidine-*N*-oxyl (carboxy-TEMPO) was coupled via DCC coupling to give polymers **4a** and **4b** respectively. Due to the paramagnetic broadening arising from the spin of the nitroxide, it was not possible to use NMR spectroscopy to determine the coupling efficiency, however GPC indicated an increase in the molecular weight of the samples, a strong EPR signal was observed and the material, while still having a significant UV absorbance, showed a strongly quenched fluorescence signal (See Table 1 for fluorescence quantum yield comparisons).

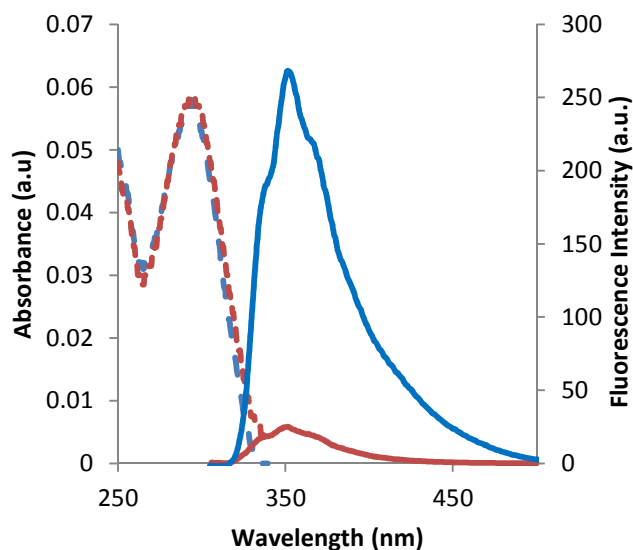


Fig. 3 Comparison of the UV-Vis absorbance (dashed lines) and fluorescence emission (solid lines) spectra of polymer **3a** (blue lines) and **4a** (red lines). Note that while the absorbance properties of the polymers is very similar, there is over 17-fold difference in the fluorescence observed once the nitroxide moiety is attached

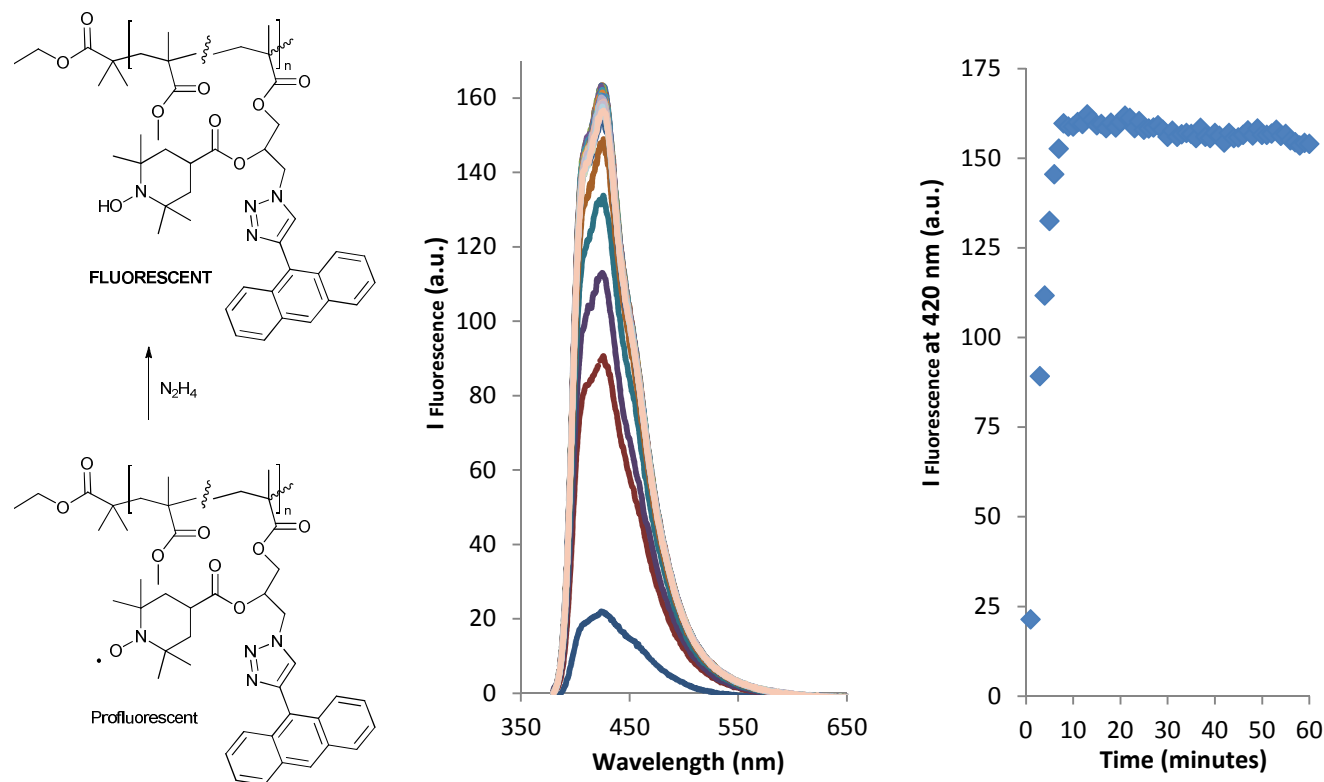


Fig. 4 Evolution of total fluorescence over time when polymer **4b** is stirred at room temperature in a solution of THF containing an excess hydrazine hydrate as a model reductant.

The attachment of 9-carboxy anthracene to polymer **3c** to yield polymer **4c** was also possible. A large increase in the UV absorbance within the GPC trace was indicative of the success of the reaction. Assuming a similar molar absorptivity to the akin, small molecule 9-methyl anthroate ($\epsilon = 7100 \text{ M}^{-1}\text{cm}^{-1}$), the coupling efficiency can be roughly estimated as ca. 70% (The molar absorptivity for polymer **4c** at 364 nm was $\epsilon = 4860 \text{ M}^{-1}\text{cm}^{-1}$).³⁷ While this is lower than the incorporation obtained for the other samples, this could be expected due to the coupling of the bulkier fluorophore employing the less efficient coupling technique. Additional steric constraints of already having the nitroxide in place may also hinder coupling.

The presence of the nitroxide moiety has a significant effect on the observed fluorescence of the polymers both in solution and in the solid state (for example see Figure 2). Preliminary studies were undertaken to assess the absorptivity and fluorescence emission of the profluorescent polymers **4a-c** compared to the fluorophore-only containing polymers **3a-b**. This data is summarized in Table 1.

Comparison of **3a** to **4a** (see Figure 3) shows the presence of the nitroxide has very little effect on the molar absorptivity or the λ_{max} of the polymers with the absorption arising due to the incorporated fluorophore. Notably however, there is a 17-fold quenching of the observed fluorescence. 10-fold quenching was observed for **4b** when comparing before and after attachment. While it was not possible to compare the fluorescence of **4c** to the polymer without the nitroxide present, comparison of the quantum yield of **4c** to **4b** shows greater than 3 times better quenching efficiency for the sample where the fluorophore is attached through click chemistry. As the molar absorptivities for the fluorophores in **4b** and **4c** are quite similar, this difference is likely to arise from greater distances between spin and fluorophore or potentially restricted non-beneficial orientations of the spin and fluorophore. Such quenching interactions have is supported by the findings Aliaga and co-workers who modelled similar systems and showed that orientation and distance play key roles in overall quenching.³⁸ The type of linkage employed could also play a significant role in the quenching. The EPR spectra suggest that when the nitroxide is attached to the polymer via CuAAC, it does not

have as much free rotation ($\tau_R = 1.25 \times 10^{-9}$ s) as when it is coupled via esterification ($\tau_R = 2.47 \times 10^{-10}$ s). Again, the amount of time spent in a non-beneficial orientation could lead to lower overall quenching. Finally, to demonstrate that the new profluorescent nitroxide containing polymers could be employed as sensor materials, solution based studies of the polymer probes were undertaken. The redox responsive properties of the polymer were examined by fluorescence emission spectroscopy in THF at a concentration where the λ_{max} of the fluorophore was optically matched to 0.1 absorbance units to ensure there was no self-quenching from the fluorophore. To this, 50 μL of hydrazine hydrate solution (1 mmol) was added and fluorescence emission was monitored over time. (See Figure 4). Hydrazine hydrate rapidly reduces the nitroxide moiety to the corresponding hydroxylamine, removing the spin. With the generation of this diamagnetic species typical fluorescence emission is returned to the polymer. As the amount of reductant added represents a large excess, complete fluorescence switch-on is observed in just 8 minutes and the signal achieved is very stable.

The polymers were also shown to be efficient sensors for the presence of carbon-centred free radicals. To demonstrate this 100 mg (ca. 0.1 mmol of profluorescent nitroxide units) of polymer **4b** were placed in a degassed solution of toluene containing 40 mg of AIBN (0.25mmol) and heated at 100 °C. Aliquots were taken periodically, cooled, optically matched via their UV absorption spectrum and the relative fluorescence emission was recorded. As shown in SI Figure S31, a steady increase in the fluorescence was observed which continued to rise until a maximum was reached after 180 minutes. Comparison to an optically matched sample of **3b** shows the fluorescence observed is ca. 89% of what would be expected from the parent fluorophore attached to the polymer backbone. This again demonstrates the efficient nature in which these materials can react with radical species, yielding non-radical diamagnetic alkoxyamines which allow fluorescence from the pendant groups to be observed.

Conclusions

Herein, we have demonstrated that profluorescent polymer sensors can be synthesised from polymers containing pendant epoxide groups utilizing orthogonal coupling chemistries. When the epoxide functionality undergoes nucleophilic ring opening, azide and hydroxyl functionalities can be introduced in close proximity. By undertaking sequential CuAAC esterification reactions, it is possible to install fluorophore and nitroxide moieties independently, but in close proximity, yielding a profluorescent polymeric material with unique properties and sensor advantages. These polymers show sensing characteristics akin to their small molecule counterparts giving rapid and efficient reactions with a reductant or with a radical source to generate diamagnetic products that reveal the inherent fluorescence response of the fluorophore within the polymers.

Acknowledgements

The authors would like to thank the ARC Centre of Excellence (CE 0561607) and the Ian Potter Foundation for financial support. ES thanks Queensland University of Technology for a postgraduate research scholarship.

Notes and references

^a School of Chemistry, Physics and Mechanical Engineering Queensland University of Technology (QUT) 2 George St, Brisbane, Queensland 4001 (Australia).

Email: j.blinco@qut.edu.au

Electronic Supplementary Information (ESI) available: [¹H NMR, FTIR, UV-Vis and fluorescence emission spectra of all polymers. EPR spectra of polymers **3c** and **4a-c**. Quantum yield of fluorescence plots for polymers **3a-b** and **4a-c**]. See DOI: 10.1039/b000000x/

- 1 L. Tebben, L. and A. Studer, *A. Angew. Chem. Int. Ed.*, 2011, **50**, 5034.
- 2 J. Nicholas, Y. Guillaneuf, C. Lefay, D. Bertin, D. Gigmes and B. Charleux, *Prog. Polym. Sci.*, 2013, **38**, 63.
- 3 B. Morrow, D. Keddie, N. Gueven, M. Lavin and S. Bottle *Free Radical Bio. Med.* 2010, **49**, 67.
- 4 J. Blinco, D. Keddie, T. Wade, P. Barker, G. George and S. Bottle *Poly. Degrad. Stab.* 2008, **93**, 1613.
- 5 N. Kahn, J. Blinco, S. Bottle, K. Hosokawa, H. Swartz, A. Micallef, *J. Mag. Res.* 2011, **211**, 170.
- 6 J. Blinco, K. Fairfull-Smith, B. Morrow and S. Bottle *Aust. J. Chem.*, 2011, **64**, 373.
- 7 N. Englert *Toxicol. Lett.* 2004, **149**, 235.
- 8 U. Franck, S. Odeh, A. Wiedensohler, B. Wehner, and O. Herbarth *Sci. Total Environ.* 2011, **409**, 4217.
- 9 M. Kleinman, C. Sioutas, and J. Froines *Inhal. Toxicol.*, 2007, **19**, 117.
- 10 L. Tecer, O. Alagha, F. Karaca, G. Tuncel and N. Eldes *J. Toxicol. Environ. Health A*, 2008, **71**, 512.
- 11 K-I. Inoue *Environ. Health Perspect.*, 2011, **119**, 446.
- 12 M. Porter, M. Karp, S. Killedar, S. Bauer, J. Guo, D. Williams, P. Breysse, S. Georas and M. Williams *Am. J. Respir. Cell. Mol. Biol.*, 2007, **37**, 706.
- 13 T. Xia, M. Knovich and A. Nel *Clin. Occup. Environ. Med.* 2006, **5**, 817. ROS
- 14 N. Surawski, B. Miljevic, B. Roberts, R. Modini, R. Situ, R. Brown, S. Bottle and Z. Ristovski *Environ. Sci. Technol.* 2010, **44**, 229.
- 15 T. Flicker and J. Green *Environ. Health Perspect.* 2001, **109**, 765.
- 16 M. Nejad, S. Green. *Arxiv.org.* 2010, DOI: arXiv:1009.2291v1.
- 17 B. Miljevic, K. Fairfull-Smith, S. Bottle, Z. Ristovski. *Atmos. Environ.* 2010, **44**, 2224.
- 18 B. Miljevic, M. Heringa, A. Keller, N. Meyer, J. Good, A. Lauber, P. Decarlo, K. Fairfull-Smith, T. Naussbaumer, A. Prevot, U. Baltensperger, S. Bottle, Z. Ristovski *Environ. Sci. Technol.* 2010, **44**, 6601.
- 19 M. Alaghmand, N. Blough. *Environ. Sci. Technol.* 2010, **41**, 2364.
- 20 M. Sleiman, H. Destailats and L. Gundel *Talanta*, 2013, **116**, 1033.
- 21 J. Blinco, J. McMurtrie and S. Bottle *Eur. J. Org. Chem.* 2007, 4638.
- 22 K. Fairfull-Smith and S. Bottle, *Eur. J. Org. Chem.* 2008, **32**, 5392.
- 23 J. Blinco, K. Fairfull-Smith, A. Micallef and S. Bottle *Polym. Chem.*, 2010, **1**, 1009.

- 24 K. Fairfull-Smith, J. Blinco, D. Keddie, G. George and S. Bottle *Macromolecules*. 2008, **41**,
- 25 K. Fairfull-Smith, S. Bottle, *Eur. J. Org. Chem.* 2008, **32**, 5391.
- 26 K. Gallas, A-C. Knall, S. Scheicher, D. Fast, R. Saf and C. Slugovc *Macro. Chem. Phys.*, 2014, **215**, 76.
- 27 J. Matko, K. Ohki, M. Edidin, *Biochemistry* 1992, **31**, 703
- 28 N. Tsarevsky, S. Bencherif, K. Matyjaszewski, *Macromolecules* 2007, **40**, 4439.
- 29 Y-S. Feng, C-Q. Xie, W-L. Qiao and H-J. Xu *Org. Lett.* 2013, **15**, 936.
- 30 T. Zdobinsky, P. Sankar Maiti and R. Klajn *J. Am. Chem. Soc.* 2013, **135**, 19135.
- 31 D. Keddie, K. Fairfull-Smith, and S. Bottle *Org. Bio. Chem.* 2008, **6**, 3135.
- 32 Q. Zhang, S. Slavin, M. Jones, A. Haddleton, D. Haddleton *Polym. Chem.*, 2012, **3**, 1016.
- 33 J. Morris, J. McMurtrie, S. Bottle, K. Fairfull-Smith *J. Org. Chem.* 2011, **76**, 496.
- 34 I. Gadwal, J. Rao, J. Baettig, A. Khan, *Macromolecules* 2014, **47**, 35.
- 35 I. Gadwal, M. Stuparu, A. Kahn *Polym. Chem.*, 2015 10.1039/c4py01453g
- 36 C. Mu, X. Fan, W. Tian, Y. Bai, Z. Yang, W. Fei. H. Chen, *Polym. Chem.*, 2012, **3**, 3330.
- 37 S. Murov, I. Carmichael and G. L. Hug, *Handbook of Photochemistry*, Marcel Dekker Inc., New York, 1993.
- 38 C. Aliaga, P. Fuentealba, M. Rezende, C. Cardenas, *Chem. Phys. Lett.* 2014, **593**, 89.